International Journal of Biological Macromolecules 79 (2015) 1004–1010

Contents lists available at ScienceDirect

International Journal of Biological Macromolecules

journal homepage: www.elsevier.com/locate/ijbiomac

Mimicking enzymatic effects of cytochrome P450 by an efficient biosensor for in vitro detection of DNA damage

Ali R. Jalalvand[a,b,d], Mohammad-Bagher Gholivand[a,*], Hector C. Goicoechea[b], Thomas Skov[c], Kamran Mansouri[d]

[a] Department of Analytical Chemistry, Faculty of Chemistry, Razi University, Kermanshah 671496734, Iran
[b] Laboratorio de Desarrollo Analítico y Quimiometría (LADAQ), Cátedra de Química Analítica I, Universidad Nacional del Litoral, Ciudad Universitaria, CC 242 (S3000ZAA), Santa Fe, Argentina
[c] Quality & Technology, Department of Food Science, Faculty of Science, University of Copenhagen, Copenhagen, Denmark
[d] Medical Biology Research Center, Kermanshah University of Medical Sciences, Kermanshah, Iran

ARTICLE INFO

Article history:
Received 19 December 2014
Received in revised form 24 May 2015
Accepted 25 May 2015
Available online 30 May 2015

Keywords:
Biosensor
Benzo(a)pyrene
DNA damage

ABSTRACT

A novel biosensor for detecting DNA damage induced by benzo(a)pyrene (BP) and its metabolite was presented in this work. The nafion-solubilized single wall carbon nanotubes-ionic liquid (SWCNTs-NA-IL) composite film was prepared and then horseradish peroxidase (HRP) and double-stranded DNA were alternately assembled on the composite film by the layer-by-layer method. The biosensor was characterized by cyclic voltammetry (CV), electrochemical impedance spectroscopy (EIS), differential pulse voltammetry (DPV), scanning electron microscopy (SEM) and computational methods. UV-vis spectrophotometry was also used to investigate DNA damage induced by BP and its metabolites in solution. The DNA biosensor was treated separately in BP, hydrogen peroxide (H_2O_2) and in their mixture, respectively. The EIS analysis showed a decrease in the charge transfer resistance at the DNA/HRP/SWCNTs-NA-IL/GCE incubated in a mixture of HRP and H_2O_2, because HRP in the presence of H_2O_2 could mimic enzymatic effects of cytochrome P450 (CYP450) to metabolize BP which could cause significant DNA damage and the exposed DNA bases reduced the electrostatic repulsion of the negatively charged redox probe and leads to Faradaic impedance changes. Finally, a novel biosensor for BP determination was developed and this method provided an indirect, and quantitative estimation of DNA damage in vitro.

1. Introduction

DNA damage induced by environmental pollutants is a major endogenous toxicity pathway in biological system [1]. Most of organic pollutants may not directly cause DNA damage, but their metabolized products by enzyme reactions are genotoxic and may cause the DNA lesion [2]. Polycyclic aromatic hydrocarbons (PAHs) are compounds, which have fused aromatic rings, and are potent atmospheric pollutants [3]. In general, the main sources of PAHs include automobile exhaust fumes and smoke from combustion of organic material [4,5]. PAHs, especially with four or more ring structures, and their metabolites, are mutagenic and toxic compounds with significant human health risk [6,7]. Benzo(a)pyrene (BP, Fig. 1A) is the basic PAH compound with five structural rings, and is classified as a potential carcinogen [8–11]. However, it was found that BP could not directly cause genetic damage; in fact, it is classified as a procarcinogen, i.e., a compound which becomes carcinogenic only after it undergoes changes by metabolic processes [12]. Generally, in vivo, BP is catalyzed by the cytochromes such as P450, to form the benzo(a)pyrene-7,8-dio-9,10-epoxide (BPDE) which is the major carcinogen causing DNA damage [13,14]. BPDE is the carcinogenic product of three enzymatic reactions (see Scheme 1) [15]: (1) BP is first oxidized by cytochrome P450 (CYP450, Fig. 1B) to form a variety of products, including (+)benzo(a)pyrene-7,8-epoxide [16]. CYP450 is a powerful catalyst, which can catalyze many types of reaction such as epoxidation and hydroxylation [17] as well as hydroxylation of the C—H bonds, even in the presence of a C=C bond [18]. Recently, it was found that horseradish peroxidase (HRP) and hydrogen peroxide (H_2O_2) could mimic CYP450 in metabolic processes, especially during epoxidation [19,20]. (2) This product is

* Corresponding author. Tel.: +98 831 4274557; fax: +98 831 4274559.
E-mail addresses: mbgholivand2013@gmail.com, mbgholivand@yahoo.com (M.-B. Gholivand).

http://dx.doi.org/10.1016/j.ijbiomac.2015.05.047
0141-8130/

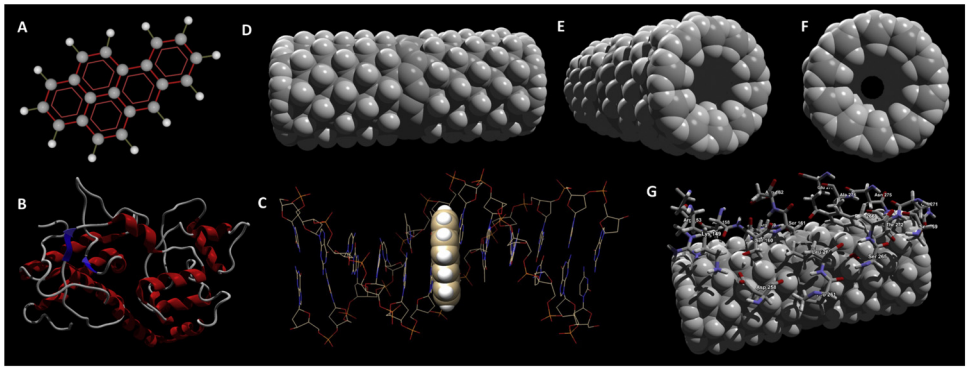

Fig. 1. (A) Molecular structure of BP. (B) Three-dimensional structure of HRP represented by solid ribbons. (C) Results of molecular docking of BPDE to DNA. (D–F) Different views of three-dimensional structure of the SWCNT designed by Nanotube Modeler software represented by the CPK model. (G) Results of molecular docking of SWCNT to HRP.

metabolized by epoxide hydrolase, opening up the epoxide ring to yield (−)benzo(a)pyrene-7,8-dihydrodiol. (3) The ultimate carcinogen is formed after another reaction with CYP450 to yield the BPDE. It is this diol epoxide that covalently binds to DNA. This molecule intercalates in DNA (Fig. 1C), and this binding distorts the DNA by perturbing the double-helical DNA structure [21]. This disrupts the normal process of copying DNA and induces mutations, which explains the occurrence of cancer after exposure. This mechanism of action is similar to that of aflatoxin which binds to the N7 position of guanine [22].

Methods for detecting DNA damage could serve as a basis for in vitro genotoxicity screening for new organic chemicals at an early stage in their commercial development. Electrochemical methods have been widely used as an in vitro model system to mimic the pathway of DNA damage in real bioprocess [23,24]. Among the electrochemical methods, electrochemical impedance spectroscopy (EIS) technique becomes increasingly popular because it offers several advantages such as simplicity, high sensitivity and serving as an elegant way to interface biorecognition events and signal transduction.

Carbon nanotubes (CNTs), attractive nanomaterials with specific electronic, chemical, and mechanical properties, can facilitate electron transfer between the electroactive species and electrode, provide a new avenue for fabricating chemical devices. Generally, carbon nanotubes exist in single-walled carbon nanotubes (SWCNTs) and multi-walled carbon nanotubes (MWCNTs). In the present

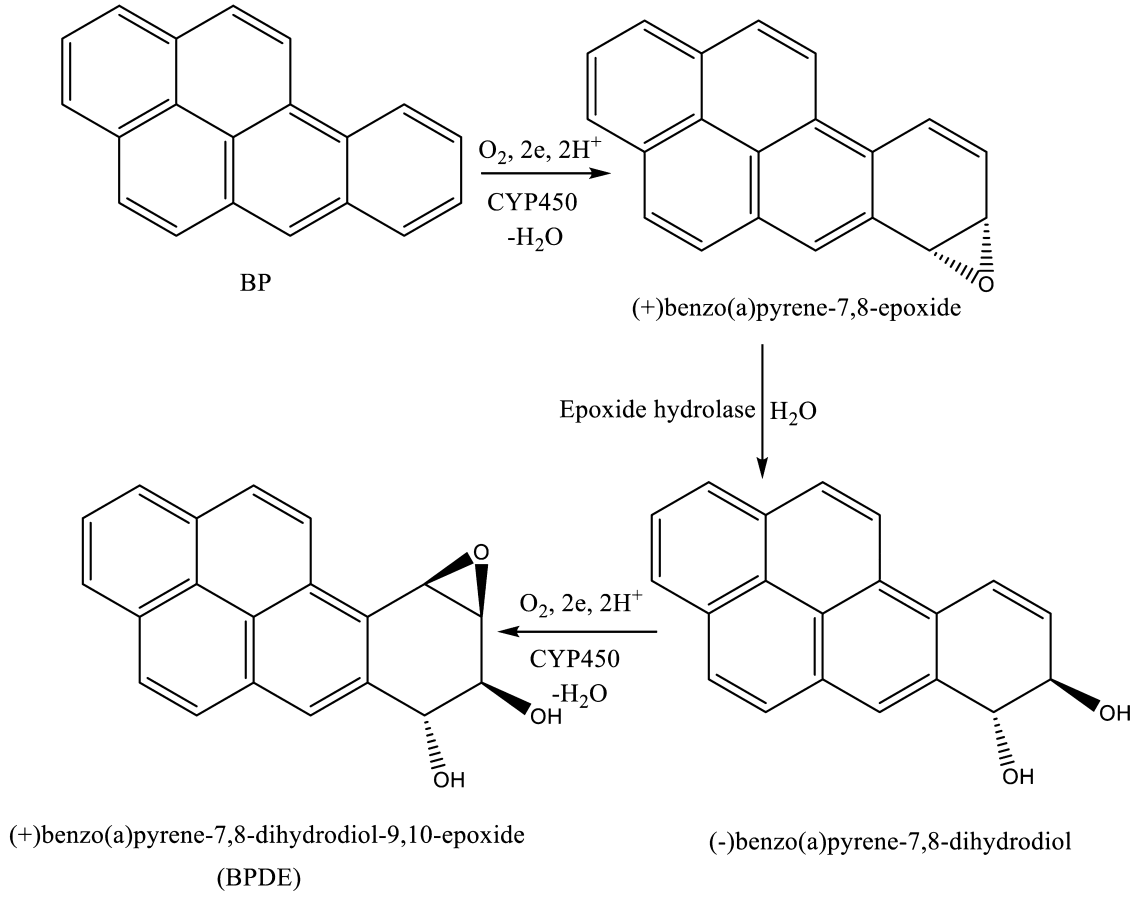

Scheme 1. Metabolism of BP by CYP450 yielding the carcinogenic benzo(a)pyren-7,8-dihydrodiol-9,10-epoxide (BPDE).

work, SWCNTs were dispersed in NA solution to form a homogenous mixture of SWCNTs-NA. In order to improve the conductivity, IL was doped into the mixture and the SWCNTs-NA-IL nanocomposite was obtained. With the isoelectric point at 8.9 [25], HRP has net positive surface charges at pH 5.5 phosphate buffer solutions. Based on this point, positively charged HRP and negatively charged DNA were assembled on the SWCNTs-NA-IL by electrostatic attraction. The SWCNTs-NA-IL nanocomposites provide a negatively charged surface for the immobilization of HRP and a biocompatible microenvironment to retain its bioactivity. After DNA/HRP/SWCNTs-NA-IL/GCE was incubated in BP or H_2O_2 or BP + H_2O_2, and DNA damage was detected by EIS based on Faradaic impedance changes. This method of directly detecting DNA damage provides a new strategy to screen the genotoxicity of new chemical pollutants and drugs in vitro. As far as we know, there are no reports on direct EIS detection of DNA damage induced by BP and its metabolite at DNA/HRP/SWCNTs-NA-IL/GCE.

2. Experimental

2.1. Chemicals and solutions

The DNA, BP, HRP, and 1-butyl-3-methylimidazolium hexafluorophosphate (IL) were purchased from Sigma and used as received. Nafion and SWCNTs were acquired from Aldrich (USA). 30% H_2O_2 solution was purchased from Sigma–Aldrich. A phosphate buffer solution (PBS, 0.1 M, pH 5.5) were prepared by mixing suitable amounts of the stock solutions of 0.1 M NaH_2PO_4 and 0.1 M Na_2HPO_4. All other chemicals were of analytical grade and used as received. A stock solution of BP (0.1 M) was prepared by dissolving a suitable amount of its crystals in dimethyl sulfoxide. A HRP solution (2.0 mg mL^{-1}) was prepared by dissolving a suitable amount of solid powder in 25 mL sodium hydroxide solution (5.0×10^{-3} M). A DNA solution (1.0 mg mL^{-1}) was prepared by dissolving 50.0 mg DNA in 50 mL 25.0 mmol L^{-1} sodium chloride solution. A fresh solution of 0.39 mol L^{-1} H_2O_2 was prepared daily. All solutions used in the experiments were adjusted with the PBS (0.1 M, pH 5.5). Doubly distilled water was used for all the preparations.

2.2. Apparatus and softwares

Electrochemical experiments were performed using a μ-AutolabIII/FRA2 controlled by the Nova software (Version 1.8). A conventional three-electrode cell was used with a saturated calomel electrode (SCE) as reference electrode, a Pt wire as counter electrode and a bare or modified GCE as working electrode. Electrochemical impedance spectroscopy (EIS) was carried out using the same three-electrode configuration above on the mentioned μ-Autolab in 5 mM $[Fe(CN)_6]^{3-/4-}$ solution containing 0.1 M KCl adjusted by the PBS (0.1 M, pH 5.5) in a frequency range from 0.1 Hz to 100 kHz. The UV–vis spectra were measured on an Agilent 8453 UV-vis Diode-Array spectrophotometer controlled by the Agilent UV-vis ChemStation software. A JENWAY-3345 pH-meter equipped with a combined glass electrode was used to pH measurements. All the recorded electrochemical data was smoothed, when necessary, and converted to data matrices by the use of several home-made mfiles in MATLAB environment (Version 7.14, MathWorks, Inc.). The three-dimensional structure of nanotubes was generated using Nanotube Modeler software (Fig. 1D–F). The chemical structure of the BP was constructed by Hyperchem package (Version 8.0), and energy minimization for BP was performed by the AM1 semi-empirical method with the Polak–Ribiere algorithm until the root mean square gradient of 0.01 kcal mol^{-1}. The molecular docking Arguslab 4.0.1 program was applied for docking studies. All the computations were performed on a DELL XPS laptop (L502X) with Intel Core i7-2630QM 2.0 GHz, 8 GB of RAM and Windows 7-64 as its operating system.

2.3. Preparation of the biosensor

The GCE was first polished to a mirror-like surface with 0.3 and 0.05 μm alumina slurry, and then sonicated successively in ethanol and doubly distilled water. Finally, the GCE was dried at room temperature for further use. In order to prepare the modified electrode, 1 mg SWCNTs was dispersed in 2 mL 0.1% NA solution with ultrasonication for 1 h to form a homogenous mixture of SWCNTs-NA. And then, 10 μL of IL was added into SWCNTs-NA solution, and continuously sonicated to obtain a homogenous SWCNTs-NA-IL

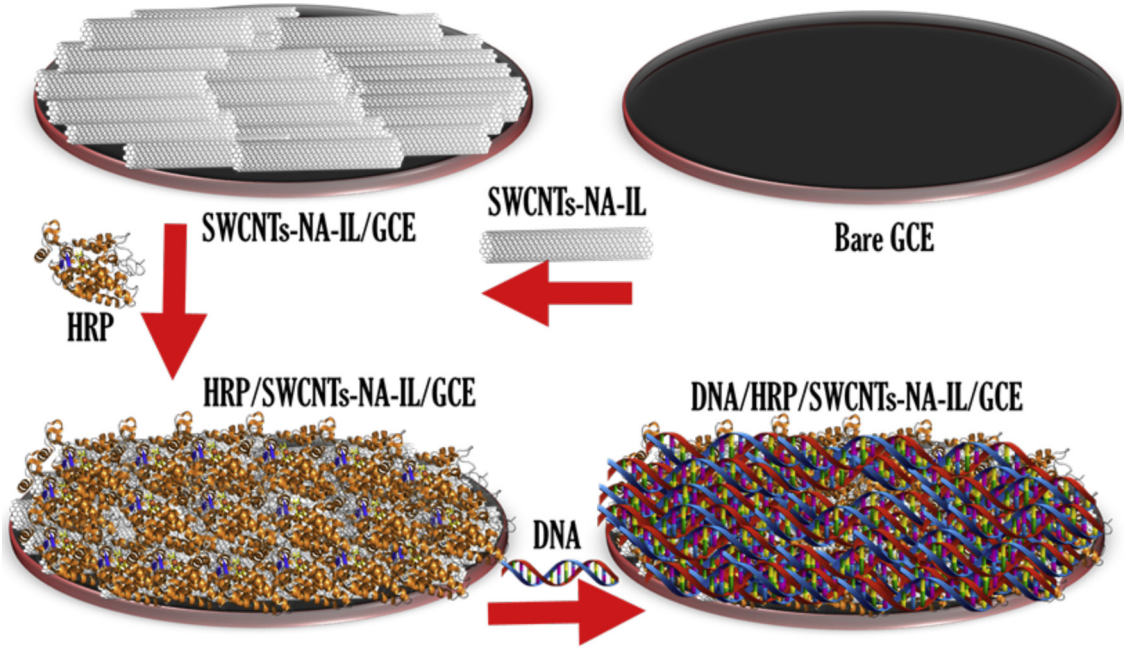

Scheme 2. Schematic representation of the fabrication procedure of DNA/HRP/SWCNTs-NA-IL/GCE.

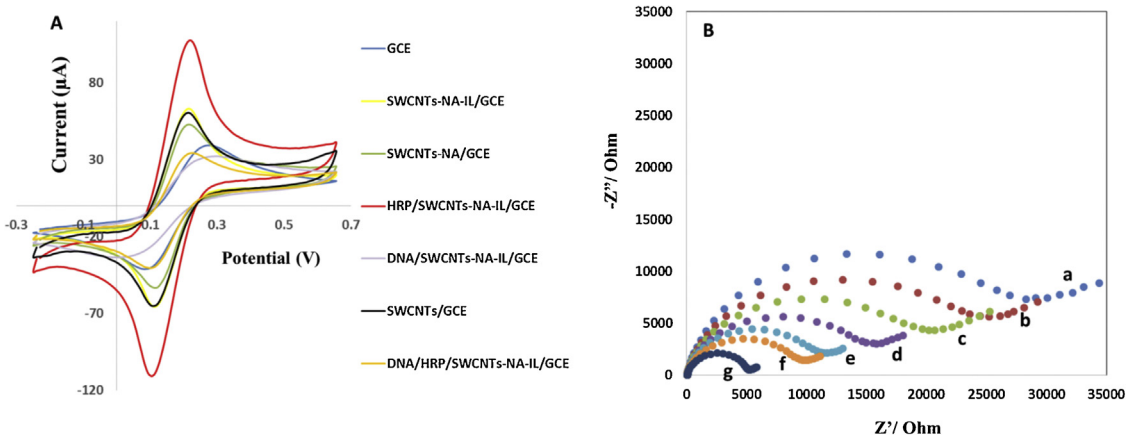

Fig. 2. In 5 mM $[Fe(CN)_6]^{3-/4-}$ solution containing 0.1 M KCl adjusted by the PBS (0.1 M, pH 5.5): (A) CVs of different modified GCEs, scan rate: 50 mV s^{-1}. (B) EISs of (a) DNA/SWCNTs-NA-IL/GCE, (b) DNA/HRP/SWCNTs-NA-IL/GCE, (c) bare GCE, (d) SWCNTs-NA/GCE, (e) SWCNTs/GCE, (f) SWCNTs-NA-IL/GCE, and (g) HRP/SWCNTs-NA-IL/GCE, the frequency range was 0.1–10^5 Hz.

solution. 6 μL of SWCNTs-NA-IL solution was dropped on the cleaned GCE surface and dried at room temperature. After that, 6 μL HRP solution (2.0 mg mL^{-1}, pH 5.5) and 6 μL DNA solution (1.0 mg mL^{-1}, pH 5.5) were alternately coated on the SWCNTs-NA-IL/GCE. Each layer was gently rinsed with doubly distilled water to remove weakly adsorbed molecules and then dried at room temperature. The obtained electrode was noted as DNA/HRP/SWCNTs-NA-IL/GCE and kept in a refrigerator at 4 °C before use. The preparation procedure is schematically illustrated in Scheme 2.

3. Results and discussion

3.1. Characterization of the prepared biosensor

3.1.1. Electrochemical characterization

The bare GCE, SWCNTs/GCE, SWCNTs-NA/GCE, SWCNTs-NA-IL /GCE, HRP/SWCNTs-NA-IL/GCE, DNA/SWCNTs-NA-IL/GCE, and DNA/HRP/SWCNTs-NA-IL/GCE were prepared and each one was characterized in 5 mM $[Fe(CN)_6]^{3-/4-}$ solution containing 0.1 M KCl adjusted by PBS (0.1 M, pH 5.5) with the use of CV (Fig. 2A). It was quite evident that a pair of well-defined redox peaks were obtained at the bare GCE and after the modification of the bare GCE with SWCNTs, the redox peak current of the electrochemical probe increased showing the enhancement in the rate of electron transfer at the SWCNTs/GCE surface. After addition of NA to SWCNTs the redox peak current of the electrochemical probe decreased and it could be attributed to the negatively charged skeleton of NA that blocked the diffusion of $[Fe(CN)_6]^{3-/4-}$ anions into the film and hindered the electron transfer. After IL was doped in SWCNTs-NA, the redox peak current of the electrochemical probe increased which could be due to the ionic conductivity of IL. After positively charged HRP and negatively charged DNA were adsorbed on the surface of SWCNTs-NA-IL/GCE, the redox peak current of the electrochemical probe increased and decreased remarkably due to electrostatic attraction between HRP and $[Fe(CN)_6]^{3-/4-}$ and electrostatic repulsion between DNA and $[Fe(CN)_6]^{3-/4-}$, respectively. After positively charged HRP and negatively charged DNA were alternatively adsorbed on the surface of SWCNTs-NA-IL/GCE, an obvious change in the redox peak current of the electrochemical probe was observed which could be ascribed to the negatively charged DNA in the (DNA/HRP) film, which blocked the electron transfer of $[Fe(CN)_6]^{3-/4-}$ with negative charge. Meanwhile, it also suggested that the (DNA/HRP) film was successfully immobilized on the SWCNTs-NA-IL/GCE.

The EIS can be used as an effective method for probing the features of interfacial electron-transfer resistance during the modification process. In the Nyquist diagram, the diameter of the semicircle reflects charge transfer resistance (R_{ct}) of redox conversion of $[Fe(CN)_6]^{3-/4-}$ at the electrode surface. The electron transfer process is caused by the presence of $[Fe(CN)_6]^{3-/4-}$ couple in the bulk solution. Any modification of the electrode surface strongly influences its electrochemistry, thus leads to a change in the R_{ct} value. When the R_{ct} is changed, then it is reflected in the change of curvature of the EIS profile, i.e., changes in the semi-circular diameters. Such changes were evident to a lesser or greater extent in the high frequency region of the EIS profiles. Therefore, further characterization of the modified electrodes immersed in the 5 mM $[Fe(CN)_6]^{3-/4-}$ solution containing 0.1 M KCl adjusted by PBS (0.1 M, pH 5.5) was performed by the EIS technique. The EIS Nyquist plots of bare GCE (Fig. 2B, curve c), SWCNTs/GCE (Fig. 2B, curve e), SWCNTs-NA/GCE (Fig. 2B, curve d), SWCNTs-NA-IL/GCE (Fig. 2B, curve f), HRP/SWCNTs-NA-IL/GCE (Fig. 2B, curve g), DNA/SWCNTs-NA-IL/GCE (Fig. 2B, curve a), and DNA/HRP/SWCNTs-NA-IL/GCE (Fig. 2B, curve b) indicated significant differences between the seven types of electrode. In this work DNA/SWCNTs-NA-IL/GCE showed the largest semi-circle which may be related to diminishing effects of the NA and DNA. This indicated that the charge on the $[Fe(CN)_6]^{3-/4-}$ probe was the most difficult to transfer from the solution to the surface of the DNA/SWCNTs-NA-IL/GCE. The smallest semi-circle was observed for HRP/SWCNTs-NA-IL/GCE which could be due to the high ionic conductivity of IL and electrostatic attraction between positively charged HRP and negatively charged electrochemical probe. These results were consistent with the conclusions from the CV analysis.

3.1.2. SEM characterization

The morphology of the as-prepared electrodes was investigated by SEM. Fig. 3A shows the SEM image of SWCNTs-IL/GCE. It confirms that SWCNTs twining around each other and aggregated on the electrode surface. Fig. 3B shows the SEM image of SWCNTs-NA-IL/GCE which confirms the role of NA on dispersing SWCNTs. Fig. 3C and D shows the SEM images of HRP/SWCNTs-NA-IL/GCE and DNA/HRP/SWCNTs-NA-IL/GCE, respectively. As can be seen the HRP adsorbed and aggregated onto the surface of the tubes and after modification of HRP/SWCNTs-NA-IL/GCE with DNA, DNA forms a thin layer on the electrode surface.

3.1.3. Computational characterization

In order to gain preliminary insights related to the interaction of HRP with SWCNTs molecular docking studies were performed to

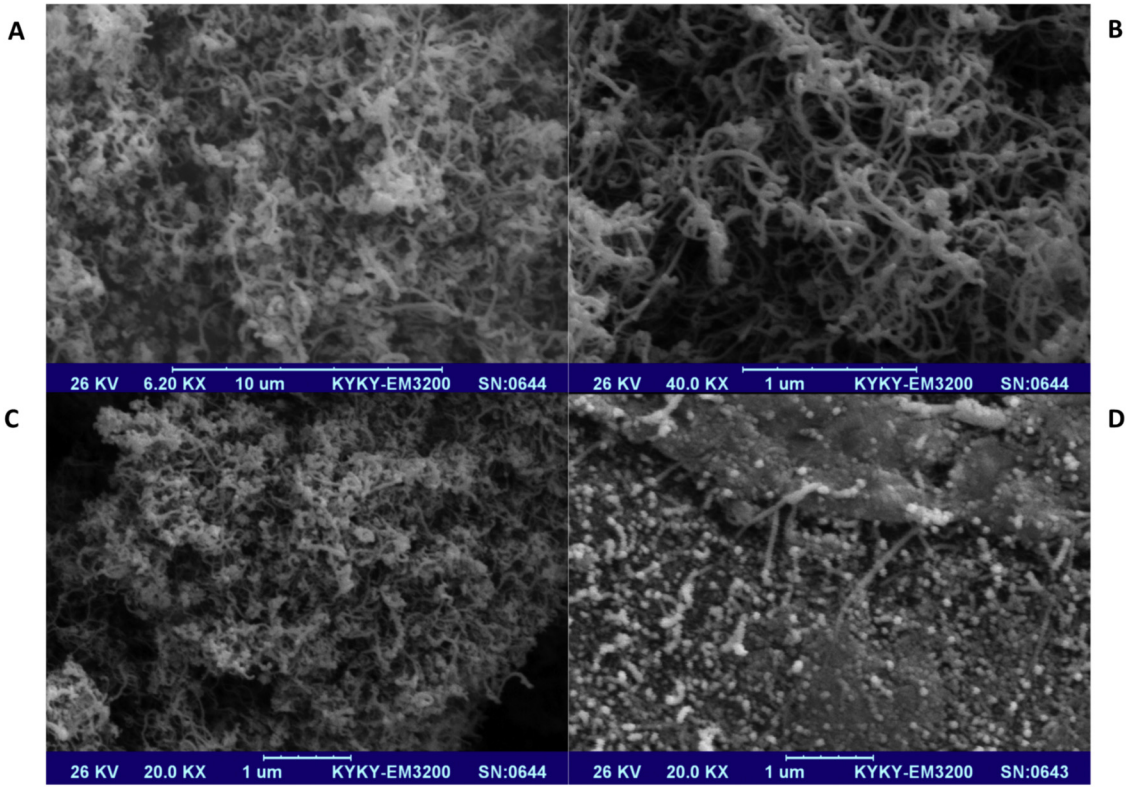

Fig. 3. SEM images of (A) SWCNTs-IL/GCE, (B) SWCNTs-NA-IL/GCE, (C) HRP/SWCNTs-NA-IL/GCE, and (D) DNA/HRP/SWCNTs-NA-IL/GCE.

identify the potential interaction sites, assuming that the SWCNTs (considered as ligand) would freely rotate around the entire structure of the HRP. Such docking studies enabled the identification of the most likely manner by which SWCNTs was bound to HRP. The docking results are shown in Fig. 1G. An additional advantage of the docking studies is the possibility to identify the HRP residues that interact the most with SWCNTs. As can be seen, SWCNTs are surrounded by Ser 269, Ser 265, Phe 266, Pro 261, Leu 262, Asp 258, Lys 149, Gln 271, Thr 272, Ser 160, Ser 161, Asn 275, Ala 276, Glu 279, Asp 162, Arg 159, Asn 158, and Arg 153. The docking of SWCNTs to HRP seems to be dominated by hydrophobic interactions. The binding constant (K_a) and free energy change (ΔG) for the binding of SWCNTs to HRP were $3.1 \times 10^5\ M^{-1}$ and $-12.31\ kJ\ M^{-1}$, respectively. Therefore, it is also reasonable to expect that the interaction of HRP with SWCNTs will be energetically favorable, leading to spontaneous formation of the nanobiocomposite which is suitable for analytical purposes.

3.2. Differential pulse voltammetric detection of DNA damage

To investigate DNA damage, which was caused by the BP metabolite, the DNA/HRP/SWCNTs-NA-IL/GCE was immersed separately in three different solutions: 0.1 μM BP, 2.0 mM H_2O_2, and 0.1 μM BP + 2.0 mM H_2O_2 for 10.0 min; thereafter, differential pulse voltammetric (DPV) analysis was performed on these treated electrodes immersed in PBS (0.1 M, pH 5.5). Fig. 4A, curve a, shows the DPV of DNA/HRP/SWCNTs-NA-IL/GCE immersed in PBS (0.1 M, pH 5.5) and no peak was observed. The possible reason for this phenomenon was that the active bases were protected by the double-stranded form of DNA and the electron transfer became very difficult to reach the electrode surface [26,27]. At the same time, it also demonstrated that DNA maintained the intact double helix under these conditions. A similar result was obtained after incubating the biosensor in 0.1 μM BP (Fig. 4A, curve b). As can be seen, there was also no any oxidation signal and this observation indicated that BP has not induced any damage to DNA because it could not be metabolized in the absence of H_2O_2. However, when the DNA/HRP/SWCNTs-NA-IL/GCE was incubated in 0.1 μM BP + 2.0 mM H_2O_2 for 10.0 min (Fig. 4A, curve c), there was an obvious peak at 0.97 V corresponding to guanine oxidation, which could be explained that the double helix of DNA was disturbed or destroyed during the incubation. These changes of DNA structure resulted from DNA damage. As can be seen, when the DNA/HRP/SWCNTs-NA-IL/GCE was immersed into a 0.2 μM BP + 2.0 mM H_2O_2 for 10.0 min which contains a higher concentration of BP a significant increase in the intensity of the anodic peak was observed (Fig. 4A, curve d). This indicated that BP could be oxidized by HRP in the presence of H_2O_2 to produce a new carcinogenic substance (BP-metabolite), which could cause significant DNA damage. Consequently, this work has indicated that BP is a typical procarcinogen, and strongly suggested that the HRP/H_2O_2 system could mimic enzymatic effects of CYP450. Thus, a new in vitro model to mimic and detect DNA damage has been successfully demonstrated.

3.3. UV-vis spectrophotometric studies on DNA damage

UV-vis spectrophotometry was carried out to investigate DNA damage induced by BP and its metabolite; also, the technique was applied to investigate the feasibility of the HRP/H_2O_2 system for mimicking enzymatic effects of CYP450 by monitoring the absorbance of DNA at 260 nm. Fig. 4B shows the UV–vis absorption spectra of 15 μg/mL DNA in PBS (0.1 M, pH 5.5) after incubation with different solutions for 12 h. DNA has an absorption at 260 nm (Fig. 4B, curve a), and after incubation with 0.5 mM H_2O_2, 2 μg/mL HRP, 2 μg/mL HRP + 0.5 mM H_2O_2, 5 μg/mL BP, 5 μg/mL BP + 0.5 mM H_2O_2, and 5 μg/mL BP + 2 μg/mL HRP shown in curves b–g of Fig. 4B, respectively, the absorbance of DNA at 260 nm were almost the same as that of curve a. It indicated that H_2O_2, HRP, HRP + H_2O_2, BP, BP + H_2O_2, and BP + HRP, could not induce DNA

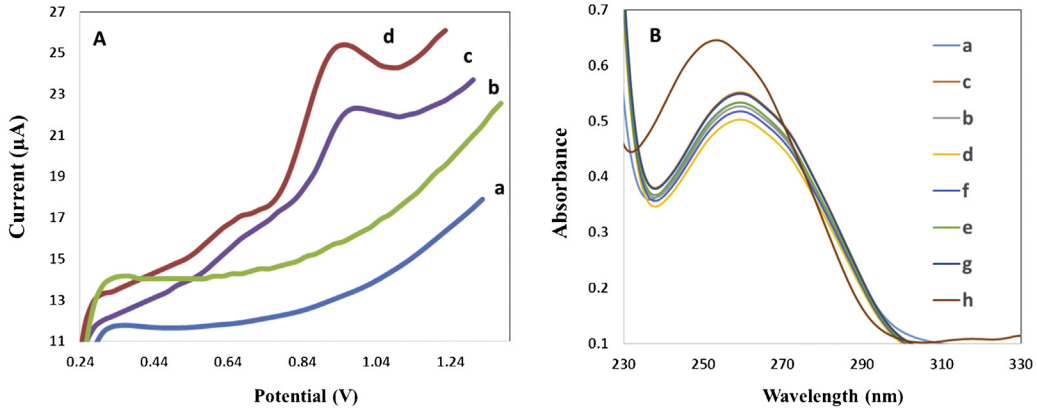

Fig. 4. (A) Differential pulse voltammograms of DNA/HRP/SWCNTs-NA-IL/GCE: (a) in PBS (0.1 M, pH 5.5) without incubation and (b–d) in PBS (0.1 M, pH 5.5) after incubation in 0.1 μM BP, 0.1 μM BP + 2.0 mM H_2O_2, and 0.2 μM BP + 2.0 mM H_2O_2 for 10.0 min, respectively. (B) The UV–vis absorption spectra in PBS (0.1 M, pH 5.5): (a) 15 μg/mL DNA, (b) 15 μg/mL DNA + 0.5 mM H_2O_2, (c) 15 μg/mL DNA + 2 μg/mL HRP, (d) 15 μg/mL DNA + 2 μg/mL HRP + 0.5 mM H_2O_2, (e) 15 μg/mL DNA + 5 μg/mL BP, (f) 15 μg/mL DNA + 5 μg/mL BP + 0.5 mM H_2O_2, (g) 15 μg/mL DNA + 5 μg/mL BP + 2 μg/mL HRP, and (h) 15 μg/mL DNA + 5 μg/mL BP + 0.5 mM H_2O_2 + 2 μg/mL HRP.

damage. However, under the existence of 5 μg/mL BP + 0.5 mM H_2O_2 + 2 μg/mL HRP, Fig. 4B, curve h, the absorbance of DNA increased significantly compared with those of curves a–g in Fig. 4B. This may be explained that during the incubation of DNA with HRP + H_2O_2 + BP, this incubation may disrupt the double helix of DNA or induce local bulges in the DNA helix, making some additional guanines inside the double-helix structure become exposed, which resulted in the increase of the absorbance of DNA at 260 nm.

3.4. EIS as an indirect method for quantitative analysis of BP

It was demonstrated that when the DNA/HRP/SWCNTs-NA-IL/GCE was immersed into the BP + H_2O_2 solution, a decrease in the R_{ct} was detected (see Section 3.1.1); this possibly occurred because the exposed DNA bases reduced the electrostatic repulsion of the negatively charged probe [28] and leads to Faradaic impedance changes. Therefore, the EIS method could be used as an indirect method for the determination of BP. For this purpose, the DNA/HRP/SWCNTs-NA-IL/GCE was immersed for 10.0 min into several solutions containing different concentrations of BP in the presence of 2.0 mM H_2O_2 adjusted by the PBS (0.1 M, pH 5.5) and then the pretreated biosensor was submitted to EIS measurements in 5 mM $[Fe(CN)_6]^{3-/4-}$ solution containing 0.1 M KCl adjusted by the PBS (0.1 M, pH 5.5). Subsequently, the relationship between $\Delta R_{ct}/R^0_{ct}$ values ($\Delta R_{ct} = R^0_{ct} - R_{ct}$, R^0_{ct}: the diameter of the semicircle of the EIS curve of DNA/HRP/SWCNTs-NA-IL/GCE in the absence of BP (Fig. 5, curve a), R_{ct}: the diameter of the semicircle of the EIS curve of DNA/HRP/SWCNTs-NA-IL/GCE in the presence of BP (Fig. 5, curves b–i)) and the concentrations of synthetic BP samples was studied (inset of Fig. 5). As shown in the inset of Fig. 5, there is a

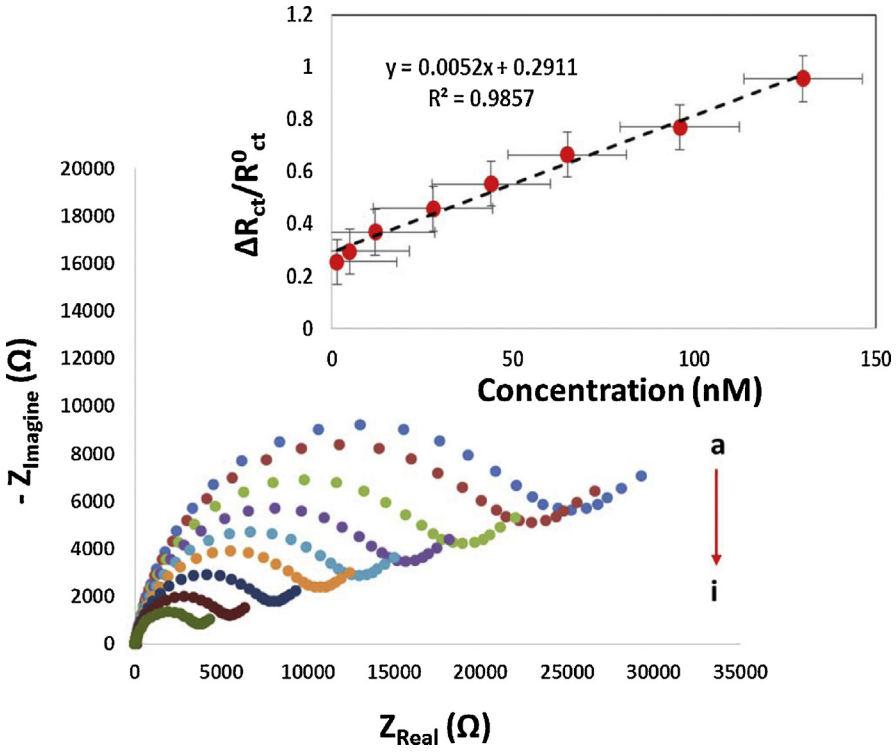

Fig. 5. The EIS curves of the DNA/HRP/SWCNTs-NA-IL/GCE in 5 mM $[Fe(CN)_6]^{3-/4-}$ solution containing 0.1 M KCl adjusted by the PBS (0.1 M, pH 5.5) after immersion for 10.0 min into several BP + H_2O_2 solutions. The solutions contain a constant concentration of H_2O_2 (2.0 mM), but different concentrations of BP including: (a) 0.0, (b) 1.5 nM, (c) 5.0 nM, (d) 12.0 nM, (e) 28.0 nM, (f) 44.0 nM, (g) 65.0 nM, (h) 96.0 nM, and (i) 130.0 nM. Inset: The corresponding calibration plot of $\Delta R_{ct}/R^0_{ct}$ versus different concentrations of BP.

Table 1
Comparison of the proposed method in this work with previous works.

Electrode	Linear range (mol L^{-1})	LOD (mol L^{-1})	Ref.
Amperometric biosensor	$3.31–16.56 \times 10^{-6}$	58.57	[29]
Boron-doped diamond electrode	$1.6–20 \times 10^{-8}$	2.86×10^{-9}	[30]
Pencil graphite electrode	$2.5–12.5 \times 10^{-7}$	2.7×10^{-8}	[31]
Mercury electrode	–	1.6×10^{-9}	[32]
DNA/hemin/nafion-graphene/GCE	$2.0–22.00 \times 10^{-8}$	1.12×10^{-8}	[26]
DNA/HRP/SWCNTs-NA-IL/GCE	$1.5–130 \times 10^{-9}$	0.65×10^{-9}	This work

linear relationship between $\Delta R_{ct}/R_{ct}^0$ and the concentration of BP over a concentration range from 1.5 nM to 130.0 nM (R^2 0.9857). The limit of detection (LOD) of this method was calculated by following IUPAC recommendations ($3S_b/b$, where S_b is the standard deviation ($n = 6$) of the blanks, and b is the slope value of the respective calibration graph) at a concentration level of 0.65 nM. For comparative purposes, Table 1 lists the linear ranges and detection limits of some other published methods for the determination of BP against the proposed method [26,29–32]. It can be seen that as compared with these published methods, linear range and LOD of this method are better. Therefore, the novel method for BP analysis, described in this work, is particularly for the determination of BP.

3.5. Stability, and reproducibility

The stability and reproducibility of a biosensor are two important parameters. The stability of the proposed biosensor was investigated by immersing it into a solution containing 20 nM BP and 2 μM H_2O_2 for 10 min and then EIS analysis was performed in the PBS (0.1 M, pH 5.5) containing 5.0 mM $[Fe(CN)_6]^{3-/4-}$. Our experiments showed that fifteen days later the response of the biosensor retained 95.6% of its initial value. This showed good stability of the biosensor. Furthermore, the reproducibility of the biosensor was examined by recording the EIS responses of six individual electrodes in the PBS (0.1 M, pH 5.5) containing 5.0 mM $[Fe(CN)_6]^{3-/4-}$ after immersing into a solution containing 20 nM BP and 2 μM H_2O_2 for 10 min and the *RSD* was got as 5.4%. This result indicated good reproducibility of the proposed biosensor.

4. Conclusions

A novel electrochemical biosensor, DNA/HRP/SWCNTs-NA-IL/GCE, was constructed with the use of the layer-by-layer method on the GCE. Computational results showed that the docking of SWCNTs to HRP seems to be dominated by hydrophobic interactions. The binding constant (K_a) and free energy change (ΔG) for the binding of SWCNTs to HRP were 3.1×10^5 M^{-1} and -12.31 kJ M^{-1}, respectively. Therefore, it was also reasonable to expect that the interaction of HRP with SWCNTs will be energetically favorable, leading to spontaneous formation of the nanobiocomposite which is suitable for analytical purposes. It was demonstrated that with the use of DPV this novel biosensor could detect the DNA damage in a solution of BP + H_2O_2, and the HRP/H_2O_2 system could mimic the enzymatic effects of the CYP450. Thus, a chemical processes in this system actually provide an in vitro model to mimic the DNA damage in vivo. The EIS and UV–vis methods were also used to detect the DNA damage induced by the BP metabolite and to test the feasibility of the HRP/H_2O_2 to mimic the enzymatic effects of the CYP450. It was demonstrated that this model system could successfully metabolize the BP to its metabolite, which facilitated the explanation of the mechanism of the DNA damage induced by BP. Subsequently, a novel, and indirect EIS method for the analysis of BP was developed based on the Faradaic impedance changes as a function of the BP concentration.

Acknowledgment

The authors gratefully acknowledge the financial support of this study by the Razi University Research Council.

References

[1] O.D. Scharer, Angew. Chem. Int. Ed. 42 (2003) 2946–2974.
[2] R.J. Turesky, Drug Metab. Rev. 34 (2002) 625–650.
[3] Y. Sapozhnikova, S.J. Lehotay, Multi-class, multi-residue analysis of pesticides, Anal. Chim. Acta 758 (2013) 80–92.
[4] Y. Segawa, D.W. Stephan, Chem. Commun. 48 (2012) 11963–11965.
[5] S. Masala, C. Bergvall, R. Westerholm, Sci. Total Environ. 432 (2012) 97–102.
[6] Z.H. Xia, X.L. Duan, S. Tao, W.X. Qiu, D. Liu, Y.L. Wang, S.Y. Wei, B. Wang, Q.J. Jiang, B. Lu, Y.X. Song, X.X. Hu, Environ. Pollut. 173 (2013) 150–156.
[7] L.H. Zhang, P.J. Li, Z.Q. Gong, A.A. Oni, J. Environ. Sci. 18 (2006) 1226–1232.
[8] International Agents for Research on Cancer (IARC), Agents Classified by the IARC Monographs, Word Health Organization, Lyon, 2011.
[9] P.W. Wester, J.J.A. Muller, W. Slob, G.R. Mohn, P.M. Dortant, E.D. Kroese, Food Chem. Toxicol. 50 (2012) 927–935.
[10] J.R. Liang, H.Y. Zhu, C.Z. Li, Y.C. Ding, Z.J. Zhou, Q. Wu, Toxicology 302 (2012) 285–291.
[11] K.P. Vijayaraman, S. Muruganantham, M. Subramanian, K.P. Shunmugiah, P.D. Kasi, Ecotoxicol. Environ. Saf. 86 (2012) 79–85.
[12] J. Padros, E. Pelletier, Mar. Environ. Res. 50 (2000) 347–351.
[13] M.L. Gao, Y.F. Li, J.G. Long, W. Shah, L. Fu, B.C. Lai, Y.L. Wang, Mutat. Res. 719 (2011) 52–59.
[14] S. Ohnishi, S. Kawanishi, Biochem. Biophys. Res. Commun. 290 (2002) 778–782.
[15] J. Hao, S.L. Gelhaus, D. Mangal, R.G. Harvey, I.A. Blair, T.M. Penning, Chem. Res. Toxicol. 20 (2007) 1331–1341.
[16] M. Shou, F.J. Gonzalez, H.V. Gelboin, Biochemistry 10 (1996) 15807–15813.
[17] A.D.N. Vaz, D.F. McGinnity, M.J. Coon, Proc. Natl. Acad. Sci. U. S. A. 95 (1998) 3555–3560.
[18] S.P. de Visser, J. Phys. Chem. B 111 (2007) 12299–12302.
[19] S. Tafazoli, P.J. O'Brien, Drug Discov. Today 10 (2005) 617–625.
[20] S.P. de Visser, S. Shaik, P.K. Sharma, D. Kumar, W. Thiel, J. Am. Chem. Soc. 125 (2003) 15779–15788.
[21] D.E. Volk, V. Thiviyanathan, J.S. Rice, B.A. Luxon, J.H. Shah, H. Yagi, J.M. Sayer, H.J. Yeh, D.M. Jerina, D.G. Gorenstein, Biochemistry 18 (2003) 1410–1420.
[22] D.L. Eaton, E.P. Gallagher, Annu. Rev. Pharmacol. Toxicol. 34 (1994) 135–172.
[23] L. Debrabandere, M. Van Boven, L. Laruella, P. Daenens, Anal. Chim. Acta 275 (1993) 295–303.
[24] M.A. García-Fernández, M.T. Fernández-Abedul, A. Costa-García, Electroanalysis 12 (2000) 483–489.
[25] Y.H. Song, L. Wang, C.B. Ren, G.Y. Zhu, Z. Li, Sens. Actuators B 114 (2006) 1001–1006.
[26] Y. Ni, P. Wang, H. Song, X. Lin, S. Kokot, Anal. Chim. Acta 821 (2014) 34–40.
[27] Y. Qiu, X. Qu, J. Dong, S. Ai, R. Han, J. Hazard. Mater. 190 (2011) 480–485.
[28] G. Ziyatdinova, J. Labuda, Anal. Methods 3 (2011) 2777–2782.
[29] Y.H. Wu, X.Q. Liu, L. Zhang, C.T. Wang, Biosens. Bioelectron. 26 (2011) 2177–2182.
[30] Y. Yardim, A. Levent, E. Keskin, Z. Senturk, Talanta 85 (2011) 441–448.
[31] E. Keskin, Y. Yardim, Z. Senturk, Electroanalysis 22 (2010) 1191–1199.
[32] A. Nelson, N. Auffret, J. Readman, Anal. Chim. Acta 207 (1988) 47–57.